ARTICLE
Journal of Cellular Biochemistry 116:1286–1299 (2015)

Journal of Cellular Biochemistry

Anti-Neuroinflammatory Effect of MC13, a Novel Coumarin Compound From Condiment Murraya, Through Inhibiting Lipopolysaccharide-Induced TRAF6-TAK1-NF-κB, P38/ERK MAPKS and Jak2-Stat1/Stat3 Pathways

Ke-Wu Zeng,[1] Qian Yu,[2] Li-Xi Liao,[1] Fang-Jiao Song,[2] Hai-Ning Lv,[1] Yong Jiang,[1]* and Peng-Fei Tu[1]*

[1]*State Key Laboratory of Natural and Biomimetic Drugs, School of Pharmaceutical Sciences, Peking University, Beijing 100191, China*

[2]*Research Studio of Integration of Traditional and Western Medicine, First Hospital, Peking University, Beijing 100034, China*

ABSTRACT

MC13 is a novel coumarin compound found in Murraya, an economic crop whose leaves are widely used as condiment (curry) in cuisine. The aims of the present study were to investigate the neuroprotective effects of MC13 on microglia-mediated inflammatory injury model as well as potential molecular mechanism. Cell viability and apoptosis assay demonstrated that MC13 was not toxic to neurons and significantly protected neurons from microglia-mediated inflammatory injury upon lipopolysaccharide (LPS) stimulation. Results showed that MC13 markedly inhibited LPS-induced production of various inflammatory mediators, including nitrite oxide (Griess method), TNF-α and IL-6 (ELISA assay) in a concentration-dependent manner. Mechanism study showed that MC13 could suppress the activation of NF-κB, which was the central regulator for inflammatory response, and also decreased the interaction of TGF-β-activated kinase 1 (TAK1)-binding protein (TAB2) with TAK1 and TNF receptor associated factor (TRAF6), leading to the decreased phosphorylation levels of NF-κB upstream regulators such as IκB and IκB kinase (IKK). MC13 also significantly down-regulated the phosphorylation levels of ERK and p38 MAPKs, which played key roles in microglia-mediated inflammatory response. Furthermore, MC13 inhibited Jak2-dependent Stat1/3 signaling pathway activation by blocking Jak2 phosphorylation, Stat1/3 phosphorylation, and nuclear translocation. Taken together, our results demonstrated that MC13 protected neurons from microglia-mediated neuroinflammatory injury by inhibiting TRAF6-TAK1-NF-κB, p38/ERK MAPKs, and Jak2-Stat1/3 pathways. Finally, MC13 might interact with LPS and interfere LPS-binding to cell membrane surface. These findings suggested that coumarin might act as a potential medicinal agent for treating neuroinflammation as well as inflammation-related neurodegenerative diseases. J. Cell. Biochem. 116: 1286–1299, 2015.

KEY WORDS: NEUROINFLAMMATION; MICROGLIA; COUMARIN; NF-κB; MAPK; JAK/STAT

Microglia, resident brain macrophages, have been proposed to play a key role in host defense and neuronal repair in the brain [Marín-Teva et al., 2011]. Under physiological conditions, microglia are involved in immune surveillance and host defense against infections [Streit and Xue, 2009]. However, under neuroinflammatory conditions, over-activation of microglia can cause brain tissue damage by releasing various cytotoxic inflammatory cytokines and further lead to neurodegenerative diseases, including Alzheimer's disease and Parkinson's disease [Tanaka et al., 2013; Amor et al., 2014]. Thus, suppression of over-activation of microglia

The authors have declared no conflict of interest.

Grant sponsor: National Key Technology R&D Program "New Drug Innovation" of China; Grant numbers: 2012ZX09301002-002-002, 2012ZX09304-005; Grant sponsor: Natural Science Foundation of China; Grant numbers: 81303253, 30873072, 81222051, 81473106.

*Correspondence to: Prof. Peng Fei Tu and Prof. Yong Jiang, State Key Laboratory of Natural and Biomimetic Drugs, School of Pharmaceutical Sciences, Peking University, Beijing 100191, China. E-mail: pengfeitu@vip.163.com (P.F. T); yongjiang@bjmu.edu.cn (Y.J)

Manuscript Received: 1 October 2014; Manuscript Accepted: 16 January 2015

Accepted manuscript online in Wiley Online Library (wileyonlinelibrary.com): 10 February 2015

DOI 10.1002/jcb.25084 • © 2015 Wiley Periodicals, Inc.

using novel pharmacological agents is an attractive issue to alleviate the neuroinflammatory processes associated with neurodegeneration, toxicology, and immunity [Rock and Peterson, 2006; Figuera-Losada et al., 2014].

At present, it is well known that lipopolysaccharide (LPS) binding to the Toll-like receptor 4 (TLR4) on the surface of microglia activates a series of complex intracellular inflammatory signaling pathways including nuclear factor-κB (NF-κB) signal [Yao et al., 2013]. NF-κB plays a key role in inflammatory diseases because NF-κB activation can induce inflammatory gene expression and further promote the production of inflammatory mediators from microglia, such as prostaglandin E_2 (PGE_2), tumor necrosis factor (TNF-α), interleukin-6 (IL-6), interleukin-1β (IL-1β), and reactive oxygen species (ROS) [Wang et al., 2012; Park et al., 2013; Dilshara et al., 2014]. Moreover, NF-κB transcriptional activity is required for TLR4-mediated interaction of TRAF6 (TNF-receptor-associated factor 6) with TAK1 (TGFβ-activated kinase 1) [Lucas and Maes, 2013]. Here, TAK1-binding protein 2 (TAB2) is an adaptator protein that brigdes TRAF6 to TAK1, promoting TAK1 activation and subsequent IκB kinase (IKK) degradation and NF-κB activation [Kenny and O′Neill, 2008]. Thus, proper regulation of NF-κB activity by targeting TLR4 adaptor proteins (TRAF6, TAB2, and TAK1) may be critical for maintaining microglial function and neuroinflammation inhibition.

Mitogen-activated protein kinases (MAPKs), as another major inflammatory signal, are also involved in regulating the expression of several inflammatory genes. Both in vitro and in vivo studies have shown that activation of MAPKs (ERK, JNK, and p38) is necessary for a number of the inflammatory responses to LPS [Lee et al., 2013; Jeong et al., 2014; Zhao et al., 2014]. For example, p38 and JNK MAPKs activities are strongly enhanced in multiple cell types including glial cells, endothelial cells, and as well as mononuclear macrophages by LPS or inflammatory cytokines through increasing their phosphorylation levels, and further accelerate inflammatory responses; moreover, TNF-α mRNA transport from the nucleus to the cytoplasm could be blocked by ERK inhibitor [Raingeaud et al., 1995; Dong and Davis, 2002; Zhi et al., 2007]. Therefore, MAPKs pathway may act as an important drug target for anti-inflammation therapy. In addition, previous research also indicated that direct LPS stimulation and LPS-induced production of IFN-γ and IL-6, which subsequently activated Janus kinase 2 (Jak2)-Stat1 and Stat3 signaling pathway, were important events for microglia-dependent neuroinflammatory process [Liu et al., 2012; Ren et al., 2013]. A negative regulation in Jak2 could effectively down-regulate Stat3 activity and suppress inflammatory mediator release. Thus, the reagents which can regulate inflammatory response through NF-κB, MAPKs and Jak/Stats pathways may be used for anti-neuroinflammation and neuroprotection.

Traditionally, curry is commonly used as food condiments in cuisine. Previous studies have shown that curry may help to prevent certain neurodegenerative diseases such as Alzheimer′s disease [Lim et al., 2001; Ringman et al., 2005; Balasubramanian 2006]. The potential mechanism might be via anti-oxidant and anti-inflammatory activity, as well as amyloid-binding capability. An important constituent of curry is Murraya, whose leaves are widely used for flavored and appetizing effects. Previously, reports suggested that the main functional ingredients of Murraya were coumarin compounds, which could exert various bioactivity, including neuroprotection, anti-cancer, anti-osteoporosis, anticoagulation, and antiviral activities [Tang et al., 2008; Riveiro et al., 2010; Bhattacharyya et al., 2011; Kontogiorgis et al., 2012; Du et al., 2014]. MC13 is a bioactive coumarin compound isolated by our group from Murraya (Fig. 1A). In this study, we found MC13 could significantly protect neurons from inflammatory injury which was mediated by microglia, the central players for inflammatory response in the brain. Moreover, we also investigated the potential anti-inflammatory mechanism of MC13 on lipopolysaccharide (LPS)-induced BV-2 microglia neuroinflammation model.

MATERIALS AND METHODS

MATERIALS

MC13 ($C_{16}H_{16}O_5$) was obtained from Department of Natural Medicines, School of Pharmaceutical Sciences, Peking University (Beijing, China). The compound was in the form of light yellow crystals, molecular weight 288 and purity over 97% by high performance liquid chromatography analysis. LPS (L6529, γ-irradiated, and BioXtra, suitable for cell culture) from *Escherichia coli* 055:B5 were from Sigma (St. Louis, MO). Alexa Fluor 488 conjugate lipopolysaccharide (LPS and L-23351) from *E. coli* Serotype 055:B5, Alexa Fluor 488 donkey anti-mouse IgG (H + L) and DyLight 594 Goat anti-rabbit IgG (H + L) were from Invitrogen (Carlsbad, CA). Fetal bovine serum (FBS), Dulbecco′s Modified Eagle medium (DMEM), antibiotics, and trypsin were from Hyclone (Logan, Utah). Primary antibodies were purchased from Cell Signaling Technology (Danvers, MA). Western Chemiluminescent HRP substrate was purchased from Pierce Scientific (Rockford, IL). NF-κB EMSA assay kit was from Beyotime Institute of Biotechnology (Jiangsu, China). TNF-α and IL-6 ELISA kits were from ExCell Bio company (Shanghai, China).

BV-2 CELL CULTURE

Murine microglial cell line (BV-2) was purchased from Peking Union Medical College, Cell Bank (Beijing, China) and cultured in DMEM supplemented with 10% fetal bovine serum, penicillin (100 U/ml), and streptomycin (100 μg/ml) in a humidified incubator containing 95% air and 5% CO_2 at 37°C.

PRIMARY MICROGLIA CULTURE

Primary microglia were isolated from the cortices of one to 3-day-old Sprague–Dawley rat Pups. Briefly, the brains (cortex tissue) were isolated, cut into 1 mm^3 species and incubated with trypsin for 30 min at 37°C. The cell suspension was seeded into culture dishes and cultured for 2 or 3 weeks in DMEM/F12 with 10% FBS. Then, the mixed glial cells were shaken at 250 rpm for 2 h at room temperature. The detached cells were seeded to obtain a homogeneous population of microglia. The purity of the microglia was 95% as determined by OX-42 immunostaining. The procedures for experimental animals were performed in accordance with the Animal Care and Use Guidelines of Peking University and the "Guide for the Care and Use of Laboratory Animals" NIH publication in 1985. All the animals were from Vital River Laboratories (Beijing, China) and acclimatized to a room with temperature (25°C) and a 12 h day–night cycle before experimentation.

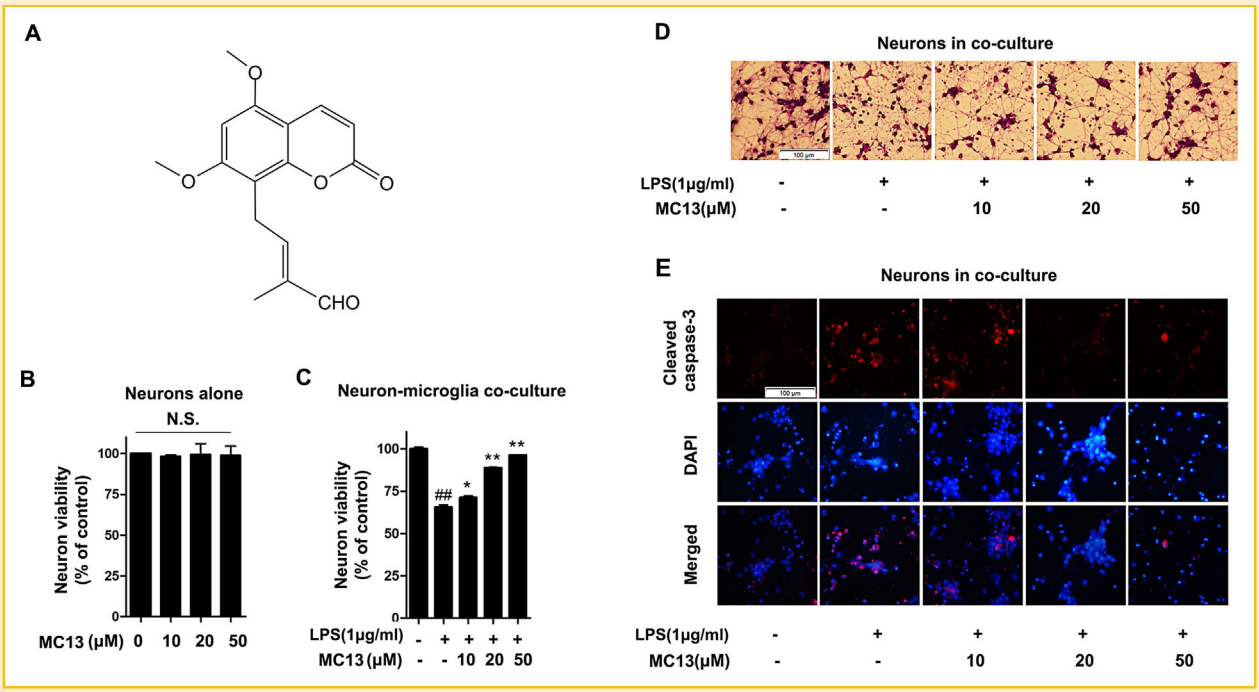

Fig. 1. MC13 protected neurons from microglia-mediated inflammatory injury. (A) The molecular structure of MC13. (B) Neurons alone culture was treated with MC13 (10, 20, and 50 μM) for 48 h, then MTT assay was done (N = 3). (C) Neuron-microglia co-culture was treated with LPS (1 μg/ml) with or without MC13 (10, 20, and 50 μM) for 48 h, then MTT assay was done for neurons (N = 3). (D) Neuron-microglia co-culture was treated with LPS (1 μg/ml) with or without MC13 (10, 20, and 50 μM) for 48 h, then crystal violet staining assay was done for neurons. (E) Neuron-microglia co-culture was treated with LPS (1 μg/ml) with or without MC13 (10, 20, and 50 μM) for 48 h, then specific cleaved caspase-3 immunocytochemistry assay was done for neurons (bar = 100 μm). Data are presented as mean ± SD from independent experiments performed in triplicate. $^{\#\#}P < 0.01$, relative to control group; $^{*}P < 0.05$, $^{**}P < 0.01$, relative to LPS group.

NEURON-MICROGLIA CO-CULTURE SYSTEM ESTABLISHMENT

Primary neurons culture was carried out as described previously [Zeng et al., 2014]. For neuron-microglia co-culture system establishment, we first seeded neurons onto 24-well culture plates for 7 days and then seeded BV-2 cells onto the inserts for 24 h, separately. Then, the BV-2-seeded inserts were moved into the wells where neurons were grown to form a neuron-microglia co-culture. In the co-culture system, the neurons and BV-2 cells could share the same growing environment but without direct interaction.

MTT ASSAY

MTT assay was used for viability detection. After treatment, MTT working solutions containing 0.5 mg/ml MTT were added into each well and incubated for 4 h at 37°C. Then, the medium was changed with the same volume of DMSO. The absorbance under 550 nm was detected and the results were expressed as the mean percentage of absorbance in treated versus control cells.

NITRITE OXIDE (NO) ASSAY

NO productions were detected by Griess method. After treatment, the culture supernatants were collected and reacted with Griess reagent (1% sulfanilamide/0.1% naphthylethylene diamine dihydrochloride/2% phosphoric acid) in a 96-well plate. Then, the optical density was detected under 540 nm with a microplate reader. Sodium nitrite was used as a standard curve in the assay

ELISA ASSAY FOR TNF-α AND IL-6

BV-2 cells were treated with LPS (1 μg/ml) for 4 h (TNF-α) and 8 h (IL-6) with or without MC13. Then, culture medium was collected and centrifuged at 16,000 rpm for 10 min. Supernatants were collected and used for detecting TNF-α and IL-6 levels by ELISA kits. TNF-α and IL-6 ELISA kits were from ExCell Bio company (Shanghai, China).

NF-κB ELECTROPHORETIC MOBILITY SHIFT (EMSA) ASSAY

NF-κB EMSA was performed with commercial Chemiluminescent NF-κB EMSA Kit (Beyotime, Jiangsu, China). Cell nuclear protein (4 μg) was incubated with biotin-labeled NF-κB probes for 20 min at room temperature. After electrophoresis on 6% native polyacrylamide gel, the gel was transferred onto positively charged nylon membrane. Then, ultra violet cross linking was performed for 15 min and the membrane was incubated with streptavidin-horseradish peroxidase conjugate for 15 min. After washes for three times, the membrane was developed with enhanced chemiluminiscent (ECL) detection solution and the images were captured by GelLogic 2200PRO imaging system (Kodak, New York, NY).

IMMUNOCYTOCHEMISTRY ASSAY

Cells were seeded on coverslips and treated with MC13 for different times. Then, the cells were fixed with 4% paraformaldehyde for 20 min followed by permeabilization (0.5% TritonX100) and

blocking (5% BSA) for 30 min at room temperature. Then, cells were incubated with primary antibody (1:250) at 4°C for overnight and then with a secondary antibody (Alexa Fluor 594, 1:500) for 1 h. The cells were further stained with DAPI (5 μg/ml in PBS) for 20 min at 37°C. After washes for three times, the cells on coverslips were sealed and images were acquired using OLYMPUS IX73 fluorescence microscope (Tokyo, Japan) with excitation/emission wavelengths of 590 nm/617 nm for Alexa Fluor-594 and 360 nm/450 nm for DAPI.

WESTERN BLOTTING

BV-2 cells were treated with MC13 for different times, and then whole cell lysates were prepared with RIPA buffer (1× cocktail inhibitor). The lysates were separated with 4–12% SDS–PAGE and transferred to PVDF membranes. The membranes were blocked with 5% non-fat milk and incubated with primary antibodies for 2 h. After being washed with PBST, the membrane was incubated with polyclonal goat anti-rabbit HRP-conjugated secondary antibody (1:1000) and incubated for 1 h at room temperature. After that, the membranes were washed with PBST and developed with an enhanced chemiluminescence (ECL) detection solution. The images were captured by GelLogic 2200PRO imaging system (Kodak).

COIMMUNOPRECIPITATION ASSAY

Coimmunoprecipitation assay was performed using 500 μg of total protein extract which was incubated with 4 μg of primary antibody at 4°C for 1 h. Then, the Sepharose A/G beads (Bioworld, USA, 20 μl) were added to the protein–antibody mixtures for 2 h at 4°C. After that, the beads were washed for six times with IP buffer and boiled with 2× SDS loading buffer for 10 min. The sample was then detected by Western blot assay.

LPS–MC13 BINDING ANALYSIS

MC13 (50 μM) was incubated with LPS (1 μg/ml) for 30 min at 37°C with a slight shaking, then the solution was centrifuged (8,000 rpm, 20 min) with centrifugal filters (Amicon Ultra 3 K membrane, Millipore Ltd. Billerica, MA). The filters could prevent LPS or MC13-binding LPS flowing into the filtrate. Then, the filtrate was detected by HPLC and MC13 peak was identified by MC13 standard. HPLC condition: Chromatographic column: ZORBAX Eclipse Plus C18; Chromatographic system: Water (A)-Acetonitrile (B); Chromatographic condition: 80% (B) to 100% (B) within 6 min; Injection volume: 100 μl, Detection wavelength: 254 nm. If MC13 cannot bind with LPS, then MC13 will be washed out and exists in filtrate, which was identified by MC13 peak in HPLC chromatogram. If MC13 can bind with LPS, then MC13 peak will become lower in HPLC chromatogram.

LPS–CELL BINDING ANALYSIS

BV-2 cells were treated with Alexa Fluor-488 conjugate-LPS for 30 min with or without MC13 (50 μM). Then, the culture medium was removed and the cells were washed with PBS for three times. The cells on coverslips were sealed and images were acquired (495 nm/519 nm for Alexa Fluor-488) using OLYMPUS IX73 fluorescence microscope (Tokyo, Japan)

STATISTICAL ANALYSIS

Data were presented as mean ± SD. Statistical analysis was performed by analysis of variance followed by the Dunnett′s test analysis using the Prism computerized package (GraphPad Software). $P < 0.05$ was considered significant.

RESULTS

MC13 PROTECTED NEURONS FROM MICROGLIA-MEDIATED INFLAMMATORY INJURY

First, we tested the toxicity of MC13 on neurons and found that MC13 (10, 20, and 50 μM) did not show any cytotoxicity based on MTT assay (Fig. 1B), indicating that MC13 was nontoxic to neurons. Then, we added MC13 into microglia-neurons co-cultures which was stimulated by LPS, and observed that LPS induced a significant neuron death through microglia-mediated inflammatory injury; however, the neuron death was concentration-dependently suppressed by MC13 treatment (10, 20, and 50 μM) (Fig. 1C). Moreover, cell morphology analysis showed that neurons sustained significant neurite injury (observed as neurite loss and cleavage) after LPS stimulation for 48 h, and MC13 markedly reversed neurite injury (Fig. 1D). Since cleaved-caspase-3 is a marker for apoptosis, we then used immunofluorescence assay to detect whether MC13 could inhibit neuron apoptosis. Figure 1E shows that LPS induced a significant increase on cleaved-caspase-3 expression (red fluorescence) which was concentration-dependently inhibited by MC13, suggesting that MC13 could inhibit neuron apoptosis against microglia-mediated inflammatory injury.

MC13 INHIBITED THE PRODUCTION OF INFLAMMATORY MEDIATORS IN LPS-INDUCED BV-2 AND PRIMARY CULTURED MICROGLIA

We treated BV-2 cells with different concentrations of MC13 (10, 20, and 50 μM) for 24 h, and found MC13 could not change BV-2 cell viability (Fig. 2A). Then, we detected the effects of MC13 on the production of various inflammatory mediators including nitrite oxide, TNF-α, and IL-6. Figure 2B–D shows that MC13 (0–50 μM) concentration-dependently decreased the production of nitrite oxide, TNF-α and IL-6 in LPS-induced BV-2 cells, indicating that MC13 exhibited a broad spectrum of inhibitory effects on the production of proinflammatory cytokines. Moreover, to verify the anti-inflammatory effects of MC13 on primary cultured microglia, we tested the inhibitory effects of MC13 on LPS-activated primary rat cortical microglia. Figure 2E–H shows that MC13 didn′t show any toxicity on rat cortical microglia, and significantly down-regulated the production of nitrite oxide, TNF-α, and IL-6 against LPS stimulation. Furthermore, we detected the effects of MC13 on the expression of inducible nitric oxide synthase (iNOS) and cyclooxygenase (COX-2), two important enzymes responsible for inflammation and pain. Figure 2I shows that treatment with MC13 effectively reduced the expression of iNOS and COX-2 in LPS-induced BV-2 cells. In order to test whether MC13 could reverse LPS-induced inflammation in other immune cells, we pretreated mouse macrophage cells (RAW264.7 cells) with LPS for 24 h in the absence or presence of MC13, and then NO production as well as the

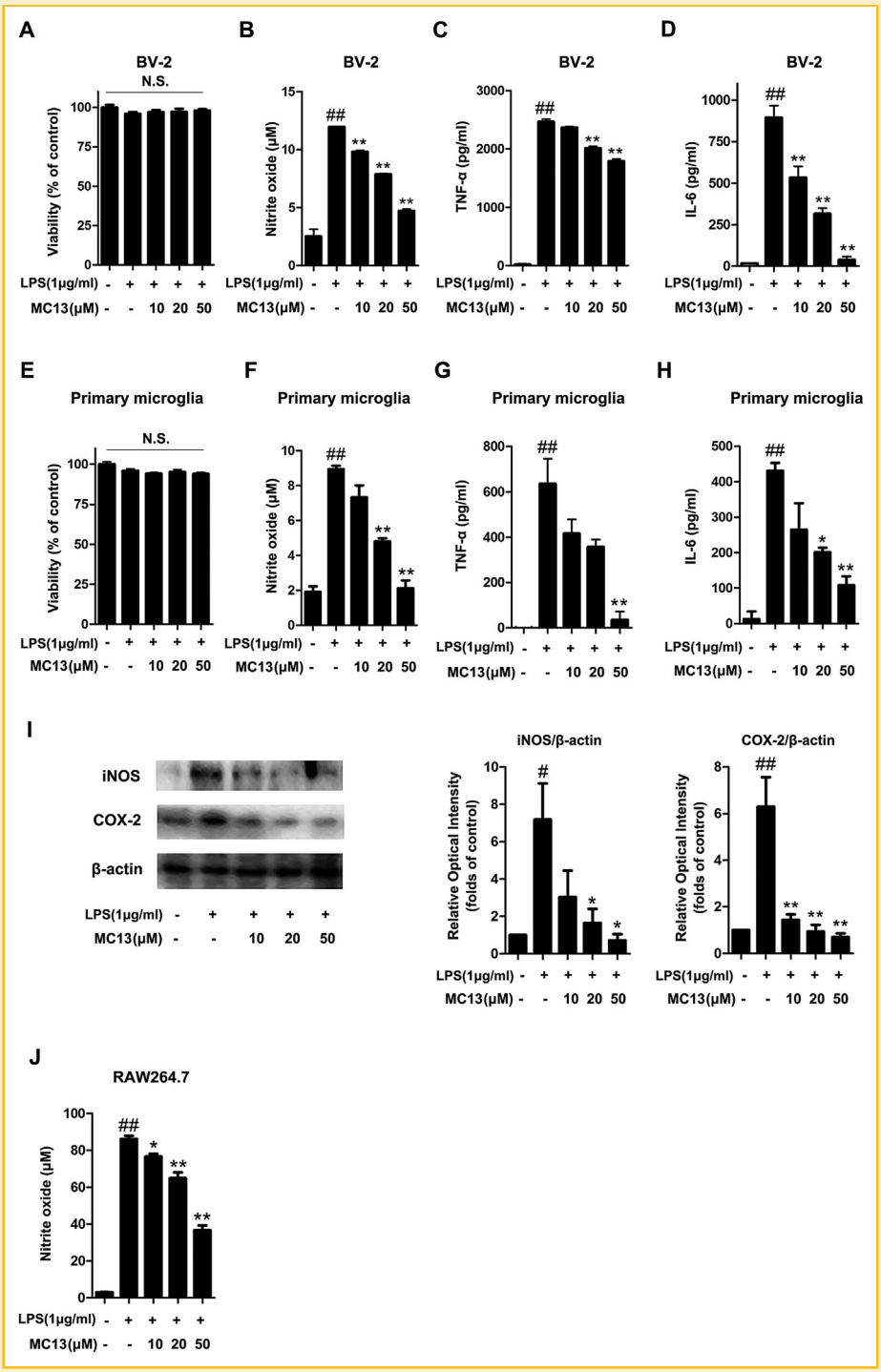

Fig. 2. MC13 inhibited the production of inflammatory mediators in LPS-induced BV-2 cells and primary cultured microglia. (A) BV-2 cells were treated with LPS (1 μg/ml) with or without MC13 (10, 20, and 50 μM) for 24 h, then MTT assay was done (N = 3). (B) BV-2 cells were treated with LPS (1 μg/ml) with or without MC13 (10, 20, and 50 μM) for 24 h, then nitrite oxide assay was done (N = 3). (C) BV-2 cells were treated with LPS (1 μg/ml) with or without MC13 (10, 20, and 50 μM) for 4 h, then TNF-α assay was done (N = 3). (D) BV-2 cells were treated with LPS (1 μg/ml) with or without MC13 (10, 20, and 50 μM) for 8 h, then IL-6 assay was done (N = 3). (E) Primary cultured microglia were treated with LPS (1 μg/ml) with or without MC13 (10, 20, and 50 μM) for 24 h, then MTT assay was done (N = 3). (F) Primary cultured microglia were treated with LPS (1 μg/ml) with or without MC13 (10, 20, and 50 μM) for 24 h, then nitrite oxide assay was done (N = 3). (G) Primary cultured microglia were treated with LPS (1 μg/ml) with or without MC13 (10, 20, and 50 μM) for 4 h, then TNF-α assay was done (N = 3). (H): Primary cultured microglia were treated with LPS (1 μg/ml) with or without MC13 (10, 20, and 50 μM) for 8 h, then IL-6 assay was done (N = 3). (I) BV-2 cells were treated with LPS (1 μg/ml) with or without MC13 (10, 20, and 50 μM) for 24 h, then Western blot assay was done for iNOS and COX-2 expression assay (N = 3).(J) RAW264.7 cells were treated with LPS (1 μg/ml) with or without MC13 (10, 20, and 50 μM) for 24 h, then nitrite oxide assay was done (N = 3). Data are presented as mean ± SD from independent experiments performed in triplicate. $^{\#}P < 0.05$, $^{\#\#}P < 0.01$, relative to control group; $^{*}P < 0.05$, $^{**}P < 0.01$, relative to LPS group.

gene expressions of inflammatory cytokines were detected. Results showed that treatment of MC13 still inhibited NO production in RAW264.7 cells (Fig. 2J); however, MC13 didn't exert any suppressive effect on the expressions of inflammatory cytokines including TNF-α, IL-6, and IL-1β (data not shown), suggesting that MC13 could exert a partly specific immunosuppressive and anti-inflammatory action on neuroimmune cells than peripheral mononuclear macrophages. To sum up, these data indicated that MC13 could concentration-dependently inhibit the LPS-induced activation of microglia, resulting in the release inhibition of neuroinflammatory mediators.

MC13 INHIBITED NF-κB PATHWAY ACTIVATION IN LPS-INDUCED BV-2 CELLS

NF-κB is a major regulator responsible for several proinflammatory mediators. Here, we investigated the nuclear translocation of NF-κB p65 subunit in LPS-induced BV-2 cells. We found that LPS induced a significant nuclear translocation of NF-κB p65; however, MC13 treatment effectively blocked this process, showing an obvious inhibitory effect on NF-κB activation (Fig. 3A). Moreover, this observation was also supported by immunofluorescence assay data via detection of intracellular location of NF-κB p50 subunit (Fig. 3B). These findings were also supported by Western blot assay, where MC13 decreased the expression of NF-κB p65 subunit in nuclear fraction and increased the expression of NF-κB p65 subunit in cytoplasm fraction (Fig. 3C). Phosphorylation of NF-κB can result in its nuclear translocation and subsequent binding with promoter regions of proinflammatory genes. We thus, explored the regulatory effects of MC13 on two major phosphorylation sites of NF-κB p65 subunit, and found that MC13 concentration-dependently decreased the phosphorylation levels of NF-κB p65 at S468 and S536 (Fig. 3D). IKK and IκB are major upstream modulators for NF-κB activation. Here, we observed that the phosphorylated protein expression of IKKα/β and IκB was significantly decreased by MC13; additionally,

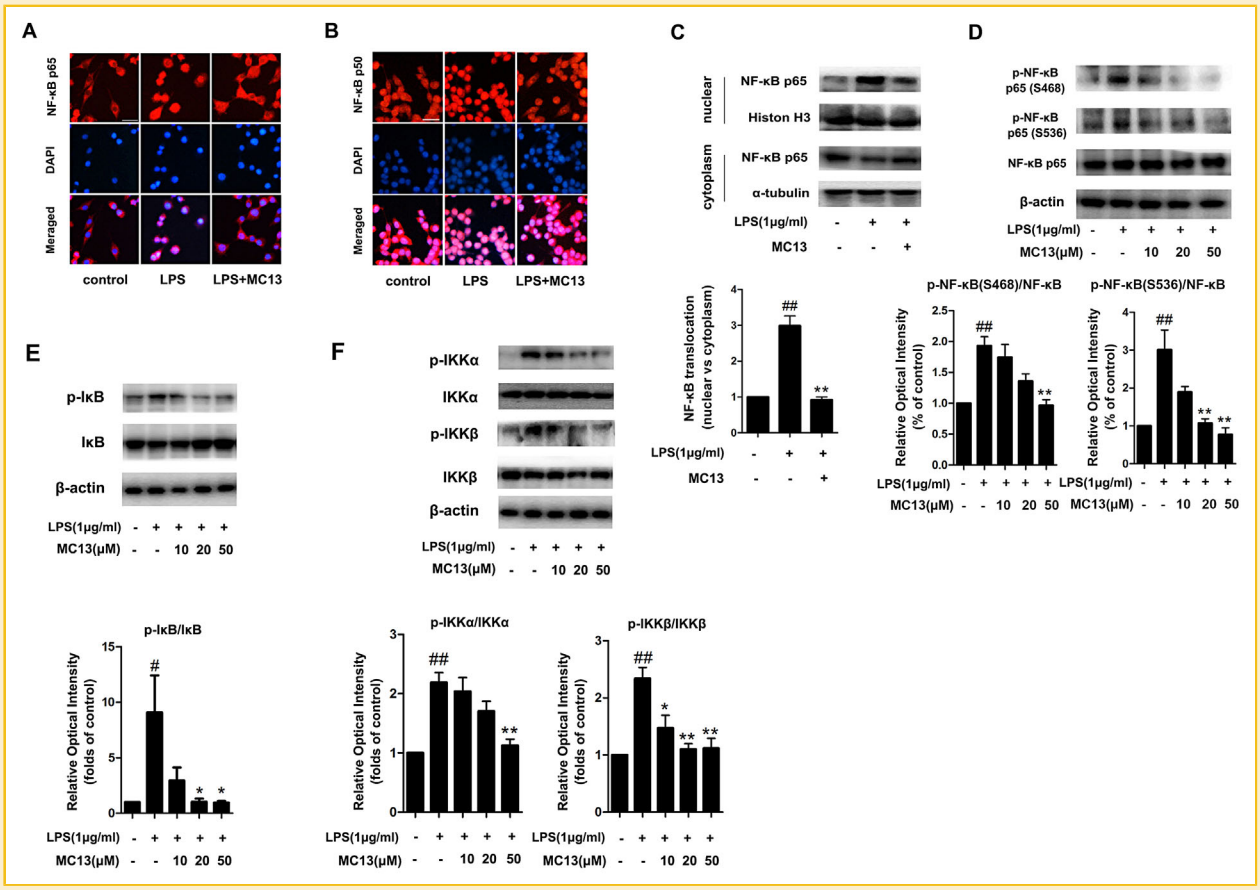

Fig. 3. MC13 inhibited NF-κB pathway activation in LPS-induced BV-2 cells. (A,B) BV-2 cells were treated with LPS (1 μg/ml) with or without MC13 (50 μM) for 1 h, then immunocytochemistry assay was done for NF-κB p65 subunit and p50 subunit translocation detection. (C) BV-2 cells were treated with LPS (1 μg/ml) with or without MC13 (50 μM) for 1 h, then Western blot assay was done for NF-κB p65 subunit translocation detection, Histon H3 was used as a nuclear protein control and α-tubulin was used as a cytoplasm protein control (N = 3). (D) BV-2 cells were treated with LPS (1 μg/ml) with or without MC13 (10, 20, and 50 μM) for 1 h, then Western blot assay was done for NF-κB p65 subunit phosphorylation assay at S468 and S536 sites (N = 3). (E) BV-2 cells were treated with LPS (1 μg/ml) with or without MC13 (10, 20, and 50 μM) for 1 h, then Western blot assay was done for IκB phosphorylation and total IκB (N = 3). (F) BV-2 cells were treated with LPS (1 μg/ml) with or without MC13 (10, 20, and 50 μM) for 1 h, then Western blot assay was done for IKKα/β phosphorylation and total IKKα/β (N = 3). Data are presented as mean ± SD from independent experiments performed in triplicate. $^{\#}P < 0.05$, $^{\#\#}P < 0.01$, relative to control group; $^{*}P < 0.05$, $^{**}P < 0.01$, relative to LPS group.

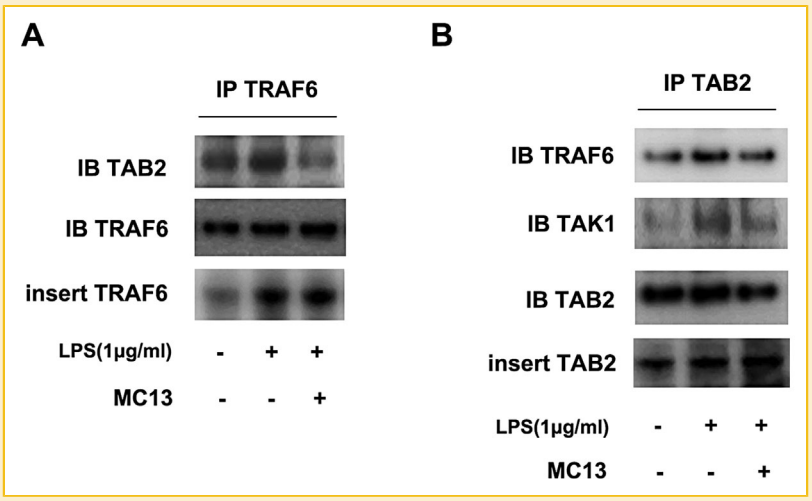

Fig. 4. MC13 blocked the interaction of TAB2 with TRAF6 and TAK1 in LPS-induced BV-2 cells. (A) BV-2 cells were treated with LPS (1 μg/ml) with or without MC13 (50 μM) for 20 min, then immunoprecipitation with antibodies against TRAF6 followed by immunoblotting with antibodies against TAB2 was performed. (B) BV-2 cells were treated with LPS (1 μg/ml) with or without MC13 (50 μM) for 20 min, then immunoprecipitation with antibodies against TAB2 followed by immunoblotting with antibodies against TAK1 and TRAF6 was performed.

the total protein expression of IκB was increased by MC13 (Fig. 3E and F), indicating that MC13 could inhibit IKK activation and IκB degradation against LPS stimulation. Taken together, these data suggested that MC13 could effectively block NF-κB activation, nuclear translocation and NF-κB-dependent proinflammatory gene activation.

MC13 BLOCKED THE INTERACTION OF TAB2 WITH TRAF6 AND TAK1 IN LPS-INDUCED BV-2 CELLS

The activation of NF-κB and IKK requires an upstream kinase complex consisting of TAK1 and adaptor proteins such as TAB2. Moreover, the association of TAK1 and TAB2 in response to TRAF6 activation, is a key signal event downstream of TLR4-dependent inflammation activation. Figure 4A shows that LPS induced the association of TRAF6 with TAB2, which was inhibited by MC13 treatment. Moreover, LPS-induced interaction of TAB2 with TAK1 was also suppressed by MC13 (Fig. 4B). These findings suggested that MC13 might inhibit the IKK-IκB-NF-κB inflammatory signaling pathway via suppressing the forming of TRAF6–TAB2–TAK1 complex.

MC13 INHIBITED P38 AND ERK MAPK ACTIVATION BUT WITHOUT JNK IN LPS-INDUCED BV-2 CELLS

MAPK signal pathway is among the most important signals that control the synthesis and release of proinflammatory mediators in microglia. Therefore, we detected the effects of MC13 on MAPK activation and found that all the phosphorylation levels of ERK, JNK, and p38 MAPK were increased upon LPS stimulation; however, MC13 significantly inhibited ERK and p38 MAPK phosphorylation, but without affecting JNK (Fig. 5A–C). These results revealed that p38 and ERK MAPK might play major roles in MC13-mediated anti-inflammation effects.

MC13 INHIBITED JAK2-STAT1/3 PATHWAY ACTIVATION IN LPS-INDUCED BV-2 CELLS

Furthermore, we explored the effects and molecular mechanisms of MC13 on Jak2/Stats signaling pathways. As shown in Figure 6A and B, LPS markedly induced nuclear translocation of Stat1 and Stat3 in LPS-stimulated BV-2 cells; however, MC13 effectively blocked these processes by increasing Stat1/3 specific red fluorescence in cytoplasm. Moreover, Western blot assay confirmed that MC13 up-regulated the expression of Stat1/3 in cytoplasm and decreased the expression of Stat1/3 in nucleus (Fig. 6C). We also investigated the phosphorylation levels of Stat1/3, as well as Jak2, a key kinase of Stat1/3. Figure 6D shows that LPS-induced high phosphorylation levels of Jak2 and Stat1/3 were markedly suppressed by MC13 treatment, suggesting that MC13 might target Jak2 and further block the activation of phosphorylated Stat1/3 and subsequent nuclear translocation.

MC13 TARGETED MULTIPLE INFLAMMATION-RELATED TARGETS, INCLUDING LPS-BINDING TO CYTOMEMBRANE RECEPTORS AND INTRACELLULAR PROTEINS

In order to find out whether MC13 could interact with LPS, we performed LPS-binding assay based on centrifugal ultrafiltration and HPLC analysis as described in methods. As a result, we found that MC13 peak (identified by HPLC in filtrate) from MC13-LPS co-incubation group became lower than MC13 alone incubation group (Fig. 7A), suggesting that MC13 might bind with LPS. Next, we treated BV-2 cell with Alexa Fluor-488-linked LPS with or without MC13, and detected whether MC13 could regulate LPS-binding with BV-2 cells. Figure 7B revealed that Alexa Fluor-488 LPS-treated cells showed strong green fluorescence compared with control (non-Alexa Fluor-488 LPS treament); however, MC13 treatment markedly down-regulated the green fluorescence,

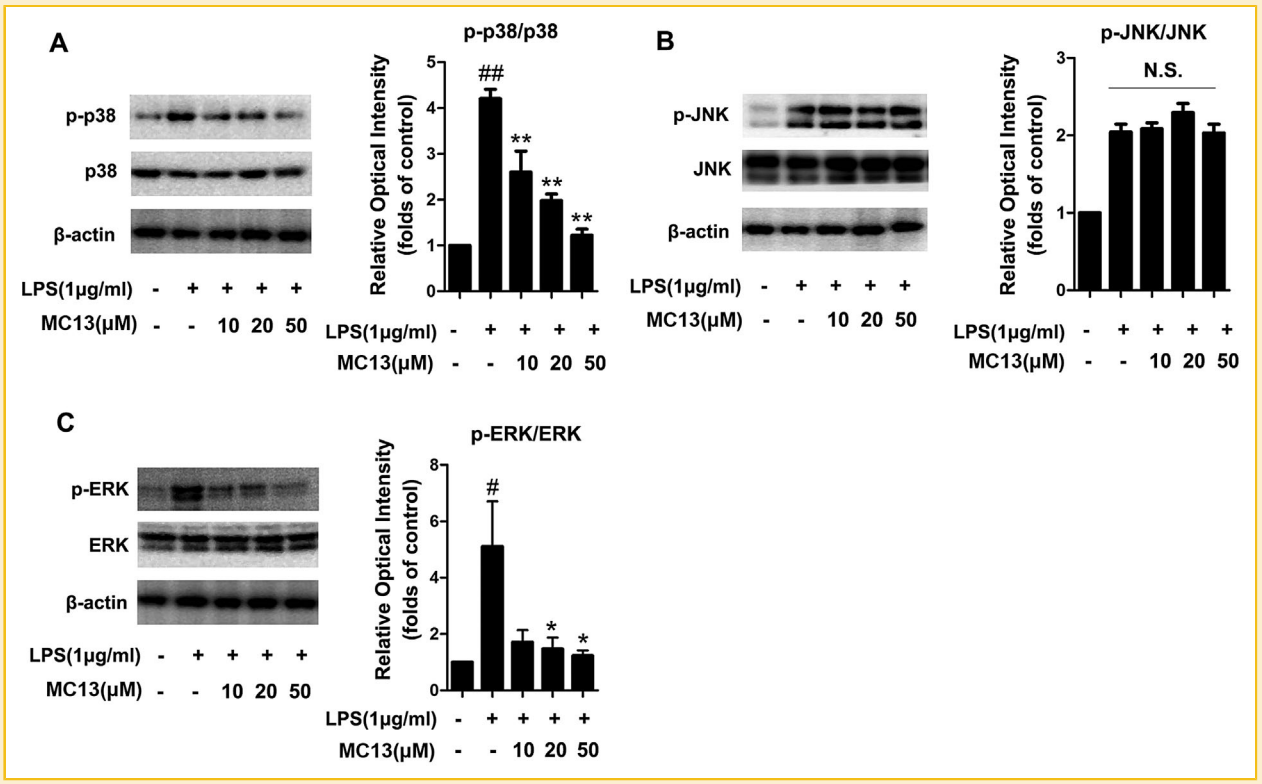

Fig. 5. MC13 inhibited p38 and ERK MAPK activation but without JNK in LPS-induced BV-2 cells. (A) BV-2 cells were treated with LPS (1 μg/ml) with or without MC13 (10, 20, and 50 μM) for 1 h, then Western blot assay was done for p38 MAPK phosphorylation and total p38 MAPK (N = 3). (B) BV-2 cells were treated with LPS (1 μg/ml) with or without MC13 (10, 20, and 50 μM) for 1 h, then Western blot assay was done for JNK MAPK phosphorylation and total JNK MAPK (N = 3). (C) BV-2 cells were treated with LPS (1 μg/ml) with or without MC13 (10, 20, and 50 μM) for 1 h, then Western blot assay was done for ERK MAPK phosphorylation and total ERK MAPK (N = 3). Data are presented as mean ± SD from independent experiments performed in triplicate. $^{\#}P < 0.05$, $^{\#\#}P < 0.01$, relative to control group; $^{*}P < 0.05$, $^{**}P < 0.01$, relative to LPS group.

suggesting that LPS-binding with BV-2 cells was effectively suppressed by MC13. Next, we established another inflammatory model by stimulating BV-2 cells with lipoteichoic acid (LTA), which was a complex component of cell walls of Gram-positive bacteria and involved in a wide range of cell processes such as the stimulation of immune responses. Then, we found MC13 could significantly inhibit No production from LTA-activated BV-2 cells, showing an effective anti-inflammation action (Fig. 7C). Since LTA-induced inflammatory response was recognized by Toll-like receptor 2 (TLR2) and further led to the activation of NF-κB; therefore, we assumed that the anti-inflammatory effect of MC13 was not only by targeting LPS–TLR4 interaction, but also acted on some downstream anti-inflammation targets shared commonly by several cytomembrane receptors such as TLR2 and TLR4. These findings suggested that MC13 might exert its anti-inflammatory actions by regulating multi-targets, which was a key characteristic of natural small molecule compounds. Moreover, to further confirm our hypothesis, we also treated BV-2 cells with LPS for 2 h to establish an activated inflammatory model, then the activated BV-2 cells were washed by PBS and further treated with MC13. Finally, we found that MC13 still showed significant inhibitory effect on NO production, suggesting that MC13 could show anti-inflammatory effect by regulating the signaling pathway downstream of LPS-TLR4 interaction (Fig. 7D). Taken together, we thought MC13 was a versatile compound via acting multiple inflammation-related targets, including cytomembrane receptors and intracellular proteins.

DISCUSSION

Our study demonstrate that (1) MC13, a bioactive coumarin compound from Murraya, protected neurons from microglia-mediated inflammatory injury; (2) MC13 inhibited microglia activation via down-regulation of various inflammatory mediators. Recent studies have shown that coumarin compounds show a variety of activities. However, the molecular mechanism by which coumarin inhibits neuroinflammatory responses in microglia still remains unknown. In our study, we found that MC13 effectively inhibited neuroinflammatory responses through blocking LPS-induced inflammation pathways, including TRAF6–TAK1–NF-κB, ERK/p38 MAPK, and Jak2-Stat1/3 pathways. These data suggested that MC13 exerted effective pharmacological activities for neuroinflammation inhibition (Fig. 8).

In brains, over-activated microglia release plenty of cytotoxic inflammatory mediators and further injury adjacent neurons [Perry and Holmes, 2014]. Therefore, effective suppression of microglia over-activation can be used as a rational therapy to treat

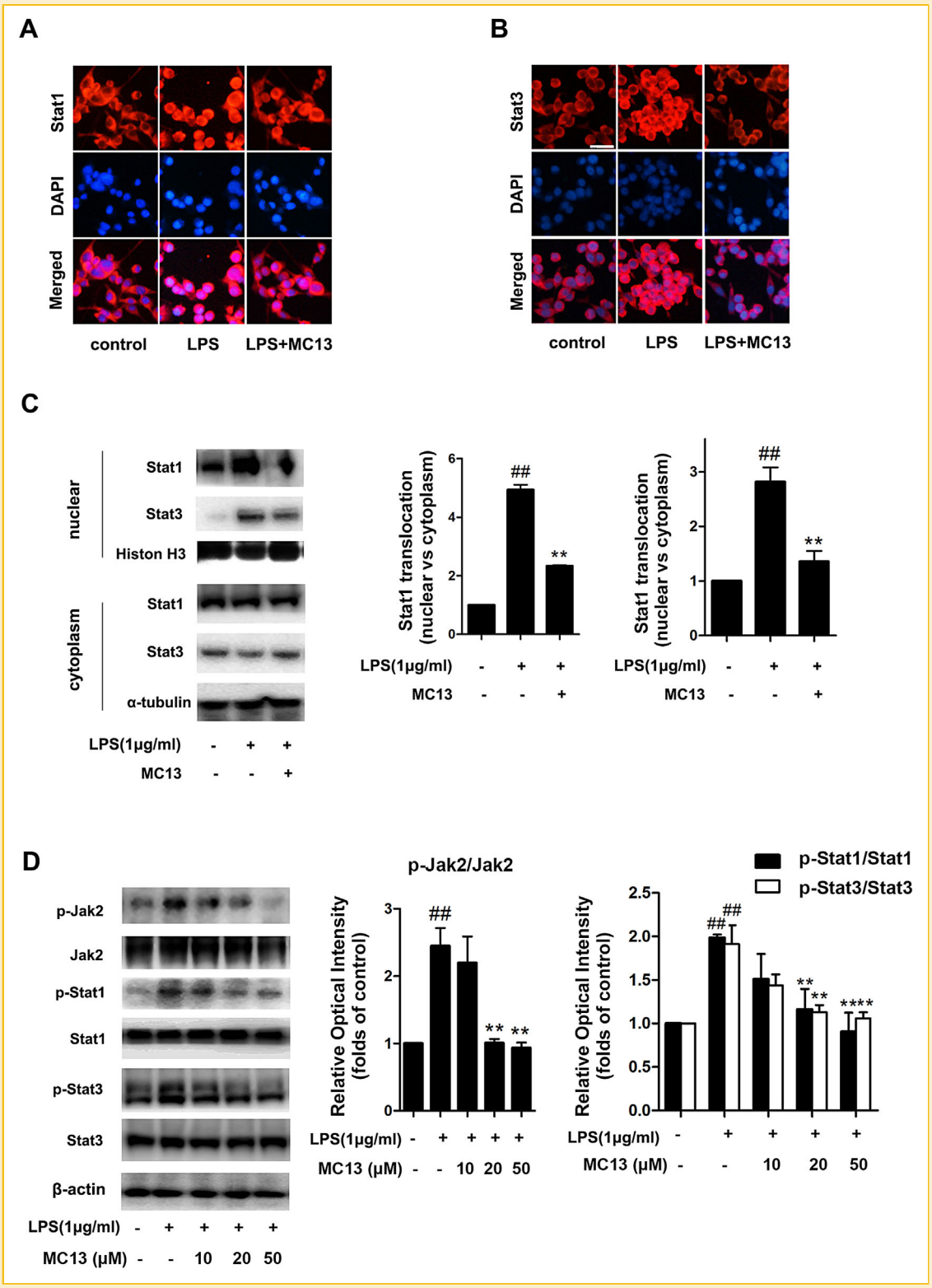

Fig. 6. MC13 inhibited Jak2-Stat1/3 pathway activation in LPS-induced BV-2 cells. (A,B) BV-2 cells were treated with LPS (1 μg/ml) with or without MC13 (50 μM) for 1 h, then immunocytochemistry assay was done for Stat3 and Stat1 translocation detection. (C) BV-2 cells were treated with LPS (1 μg/ml) with or without MC13 (50 μM) for 1 h, then Western blot assay was done for Stat1/3 translocation detection, Histon H3 was used as a nuclear protein control and α-tubulin was used as a cytoplasm protein control (N = 3). (D) BV-2 cells were treated with LPS (1 μg/ml) with or without MC13 (10, 20, and 50 μM) for 1 h, then Western blot assay was done for Jak2, Stat1, and Stat3 phosphorylation assay (N = 3). Data are presented as mean ± SD from independent experiments performed in triplicate. $^{\#}P < 0.05$, $^{\#\#}P < 0.01$, relative to control group; $^{*}P < 0.05$, $^{**}P < 0.01$, relative to LPS group.

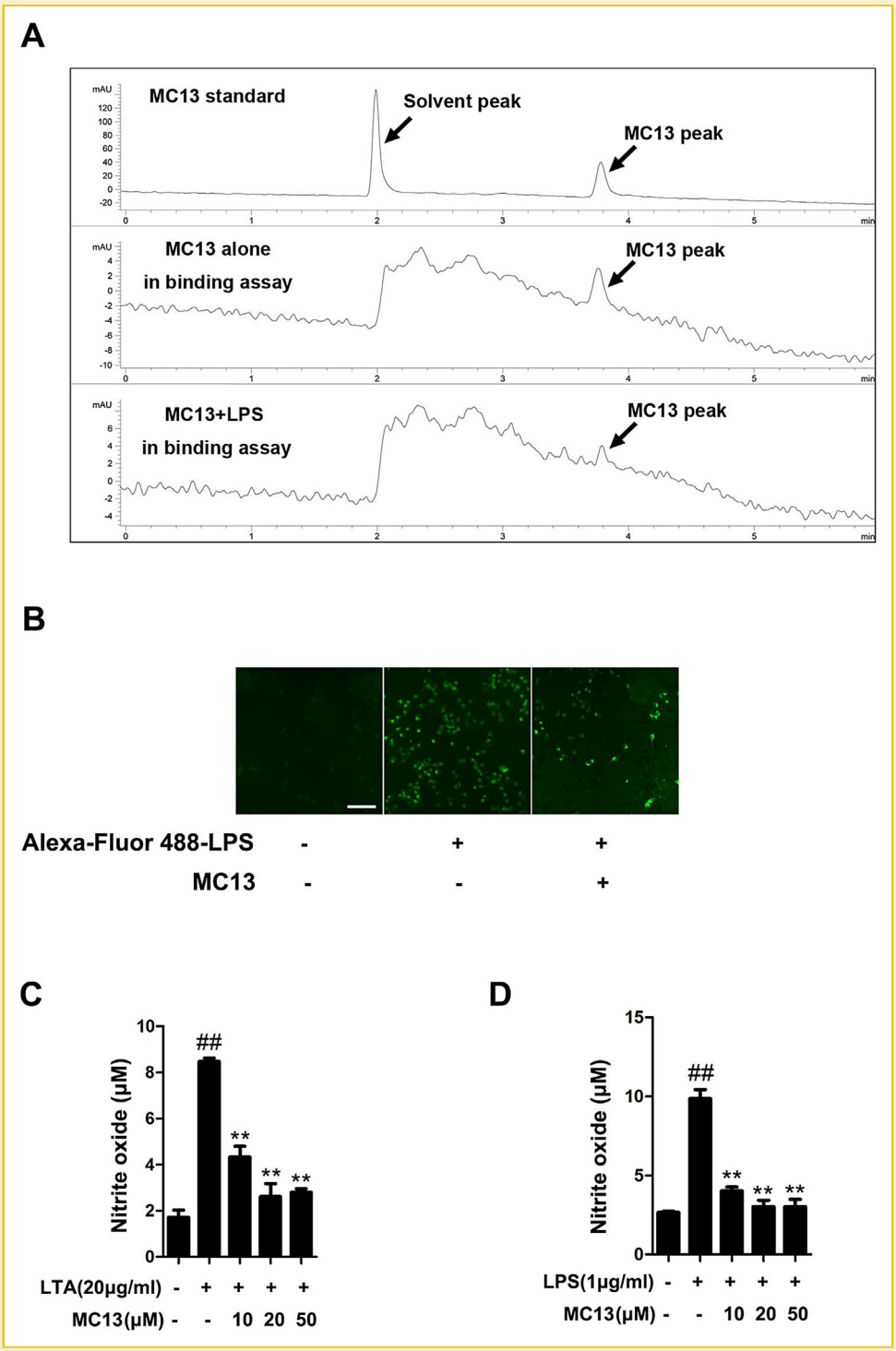

Fig. 7. MC13 interacted with LPS and block LPS-binding to BV-2 cells. (A) MC13 (50 μM) was incubated with LPS (1 μg/ml) for 30 min at 37°C, then the solution was centrifuged (8,000 rpm, 20 min) with centrifugal filters. Then, the filtrate was detected by HPLC and MC13 peak was identified by MC13 standard. (B) BV-2 cells were treated with Alexa Fluor-488 conjugate-LPS for 30 min with or without MC13 (50 μM). Then, the cells on coverslips were sealed and images were acquired using fluorescence microscope. (C) BV-2 cells were treated with LTA (20 μg/ml) with or without MC13 (10, 20, and 50 μM) for 24 h, then nitrite oxide assay was done (N = 3). (D) BV-2 cells were firstly treated with LPS (1 μg/ml) for 2 h, then cells were washed and further treated with MC13 (10, 20, and 50 μM) for another 24 h. Nitrite oxide assay was done (N = 3). Data are presented as mean ± SD from independent experiments performed in triplicate. $^{\#\#}P < 0.01$, relative to control group; $^{*}P < 0.05$, $^{**}P < 0.01$, relative to LTA or LPS group.

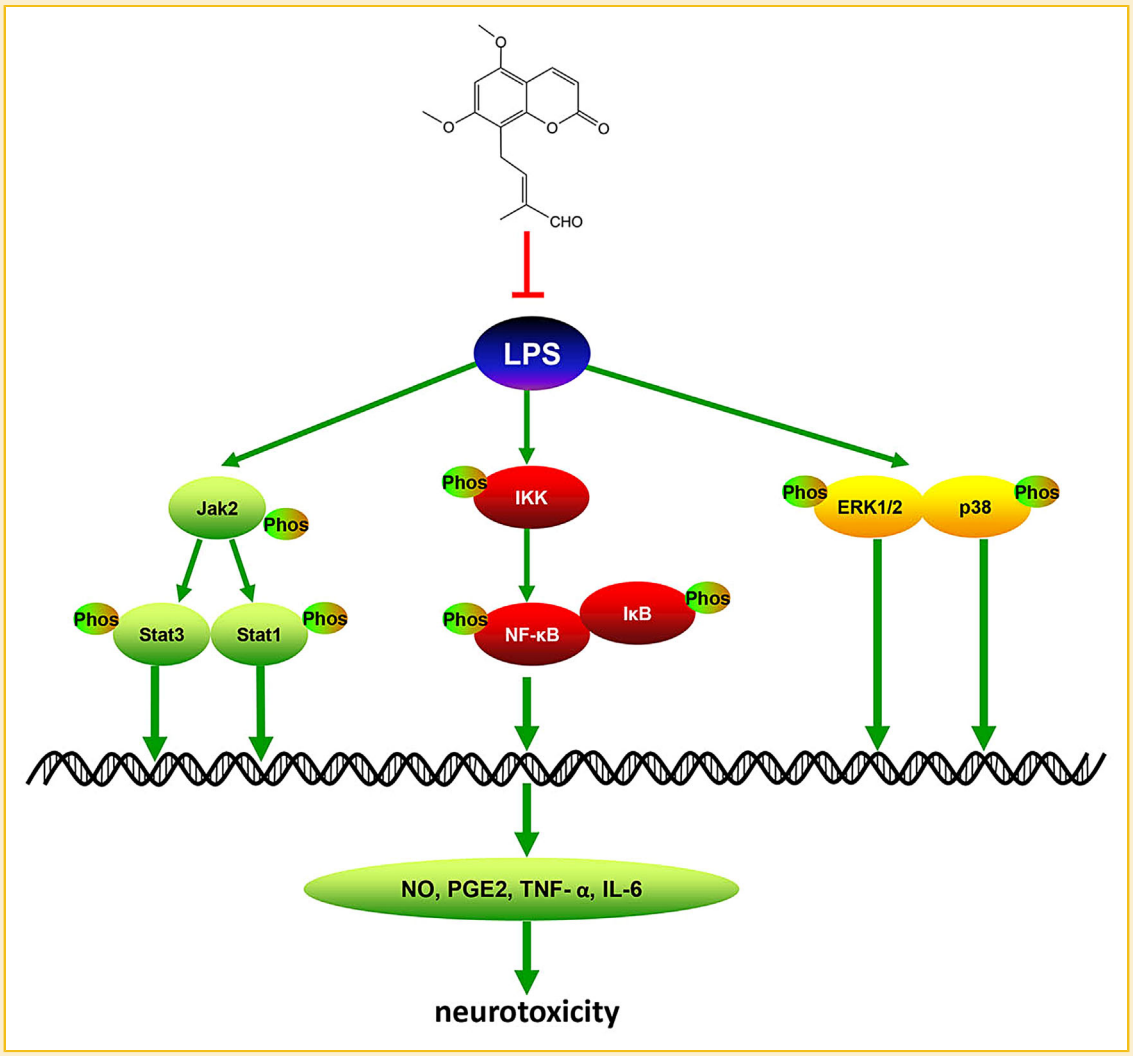

Fig. 8. Mechanism of MC13-mediated anti-neuroinflammatory effects against LPS insult.

neuroinflammation and inflammation-related neuronal injury [Morales et al., 2014]. Our study demonstrated that MC13 could significantly increase the viability of neurons (MTT assay) and inhibit neuron apoptosis (marked by cleaved caspase-3) against microglia-mediated inflammatory damages by down-regulating various inflammatory mediators including NO, TNF-α, and IL-6. Since all of these inflammatory mediators belong to potent inducers of neurotoxic and oxidation events, thus the neuroprotective effects of MC13 was likely achieved by attenuating the release of these mediators. It is worth to point out that MC13 didn′t show any effects on the viability of neurons alone culture (MTT assay), suggesting that this compound is non-neurotoxic and safe. Another point is worthy of being mentioned that, MTT assay data usually represent an indirect correlation with cell viability. Because MTT assay is mainly based on detecting mitochondrial activity, if the agents or compounds can seriously affect mitochondrial function, then the MTT assay result will not really represent cell viability.

Here, we observed that the regulatory effect of MC13 on iNOS and COX-2 is somewhat different from TNF-α and IL-6. This might be resulted from that MC13 which showed different regulatory actions on different proteins synthesis process from mRNA, which led to the differences among various inflammatory gene expressions. Moreover, we speculated that the differences in different inflammatory mediator expressions were also resulted from several diverse inflammatory signaling pathways such as NF-κB, Jak-Stat, and MAPK pathways. Of course this needs future investigation. Furthermore, from our data, we thought primary microglia and BV-2 cells showed similar response to MC13-regulated inflammatory mediators′ expressions except for TNF-α. Interestingly, we found that MC13 showed more significant inhibitory effects on TNF-α expression on primary microglia than BV-2 cells, suggesting that MC13 might exert preferable therapeutic action on inflammatory response in brains, because the physiological characteristics of primary microglia are closer to in vivo biological environments than BV-2 cells.

The production of large quantities of neuroinflammatory mediators may contribute to the pathophysiology of neuroinflammation [Rubio-Perez and Morillas-Ruiz, 2012]. NF-κB, as an important drug target for anti-inflammation therapy, regulates various inflammatory gene productions [Shu et al., 2014]. In response to LPS stimulation, the association of TAK1 and TAB2 is able to induce IKK phosphorylation and IκB degradation, which results in NF-κB activation [Imani et al., 2011]. During this process, TRAF6 firstly acquires sensitive signal from LPS-stimulated toll-like receptor 4 (TLR4) and associates with TAK1 and TAB2 to form protein complex. This complex further activates the downstream of NF-κB signaling pathway [Brown et al., 2011]. In our research, we found that MC13 could inhibit the interaction of TRAF6 with TAB2 as well as the interaction of TAK1 with TAB2. This might cause an inhibitory effect on IKK phosphorylation, IκB degradation, and NF-κB activation. Interestingly, we actually observed that MC13 markedly decreased the IKK phosphorylation and IκB degradation. In addition, MC13 also inhibited the nuclear translocation of NF-κB. These findings showed that MC13 exerted an effective anti-inflammatory activity via suppressing TRAF6–TAB2–TAK1 complex formation, leading to NF-κB signaling pathway blockage in LPS-induced BV-2 cells.

The induction of inflammatory factor production involves the activation of multiple signal transduction pathways, including mitogen-activated protein kinases (MAPKs) such as p38, ERK, and JNK [Kim et al., 2004]. Here, we focused on the roles of MAPKs as signal transduction mediators and examined the evidence linking p38, ERK and JNK to the anti-inflammatory effects of MC13 in BV-2 cells. We found that MC13 specifically down-regulated the phosphorylation levels of p38 and ERK against LPS stimulation. In addition, MC13 did not show any effects on JNK phosphorylation in LPS-induced BV-2 cells. Previous reports showed that ERK MAPK was usually activated in response to growth factors stimulation, while p38 MAPK was responsive to stress stimuli; moreover, the cross-talk between p38 and ERK MAPK has also been reported [Qu et al., 2012; Li et al., 2013]. Therefore, we speculated that MC13 might mediate a common upstream regulator or kinase of ERK and p38 MAPKs, finally leading to the inhibition of ERK and p38 MAPKs. Of course, this needs further investigation.

Jak2 belongs to the Jak family and the major substrate for Jak2 is the family of Stats, including Stat1 and Stat3. Jak2 transduces the LPS-induced signals to downstream molecules to activate the phosphorylation and nuclear translocation of Stat1/3, leading to the expression of proinflammatory genes [Qi et al., 2013; Saravanan et al., 2014]. In this study, we observed that LPS stimulation induced obvious up-regulation of Jak2 phosphorylation and resulted in the nuclear translocation of Stat1/3. This observation suggested that LPS could directly induce Jak2 activation or through LPS-dependent IFN-γ or IL-6 stimulation. In addition, we also found that this process was markedly reversed by MC13 by down-regulating Jak2 phosphorylation and Stat1/3 nuclear translocation. This observation indicated that MC13 could block Jak2 activation and inhibit Jak2-Stat1/3 pathway to restrain inflammatory mediator production.

Finally, we investigated whether MC13-dependent inflammation signaling pathways suppression was resulted from MC13-mediated blockage on LPS-binding to BV-2 cells. Interestingly, we found that MC13 could interact with LPS which was verified by LPS-binding assay. Moreover, MC13 could block LPS-binding to BV-2 cells in fluorescence labeling assay. These observations suggested that MC13 might interact with LPS and further interfere LPS translocation and binding to cell surface, which leads to the subsequent inflammation pathways suppression.

MC13 belongs to coumarin compound and this kind of structure usually shows well immunoregulatory and neuroprotective effects as well as the capacity passing through BBB (blood–brain barrier). For example, previous report showed that osthole was a natural coumarin which could improve neurobehavioral functions in vivo and reduce infarct volume in transient focal cerebral ischemia model [Mao et al., 2011]. In addition, osthole can also effectively treat experimental autoimmune encephalomyelitis in C57 BL/6 mice model [Chen et al., 2010]. Interestingly, the basic molecular structure of MC13 and osthole was the same, except for two substituent groups (Fig. 1). Thus, we speculated that MC13 might be able to pass BBB and exert similar anti-neuroinflammatory effects in vivo as well. Moreover, another report showed that coumarin derivative 20 (with similar mother molecular structure as MC13) exhibited effective neuroprotection in middle cerebral artery occlusion rats by improving neurological function and suppressing neuronal loss. Particularly, pharmacokinetic evaluation indicated that coumarin derivative 20 could penetrate BBB of rats [Sun et al., 2013]. Therefore, we assumed that MC13 might own similar capacity like coumarin derivative 20 passing BBB. Of course, these conclusions need comprehensive and systematic pharmacokinetics study in the future.

Taken together, we presented evidence that the coumarin compound MC13 exerted anti-microglial and anti-neuroinflammatory effects, and MC13 might be developed into broad spectrum anti-neuroinflammation drugs via targeting several inflammatory signaling pathways.

ACKNOWLEDGMENTS

This work was supported by grants from the National Key Technology R&D Program "New Drug Innovation" of China (No. 2012ZX09301002-002-002 and 2012ZX09304-005) and the Natural Science Foundation of China (Nos. 81303253, 30873072, 81222051, and 81473106).

REFERENCES

Amor S, Peferoen LA, Vogel DY, Breur M, van der Valk P, Baker D, van Noort JM. 2014. Inflammation in neurodegenerative diseases—An update. Immunology 142:151–166.

Balasubramanian K. 2006. Molecular orbital basis for yellow curry spice curcumin′s prevention of Alzheimer′s disease. J Agric Food Chem 54:3512–3520.

Brown J, Wang H, Hajishengallis GN, Martin M. 2011. TLR-signaling networks: An integration of adaptor molecules, kinases, and cross-talk. J Dent Res 90:417–427.

Bhattacharyya SS, Paul S, De A, Das D, Samadder A, Boujedaini N, Khuda-Bukhsh AR. 2011. Poly (lactide-co-glycolide) acid nanoencapsulation of a synthetic coumarin: Cytotoxicity and bio-distribution in mice, in cancer cell

line and interaction with calf thymus DNA as target. Toxicol Appl Pharmacol 253:270–281.

Chen X, Pi R, Zou Y, Liu M, Ma X, Jiang Y, Mao X, Hu X. 2010. Attenuation of experimental autoimmune encephalomyelitis in C57 BL/6 mice by osthole, a natural coumarin. Eur J Pharmacol 629:40–46.

Dilshara MG, Lee KT, Jayasooriya RG, Kang CH, Park SR, Choi YH, Choi IW, Hyun JW, Chang WY, Kim YS, Lee HJ, Kim GY. 2014. Downregulation of NO and PGE2 in LPS-stimulated BV2 microglial cells by trans-isoferulic acid via suppression of PI3K/Akt-dependent NF-κB and activation of Nrf2-mediated HO-1. Int Immunopharmacol 18:203–211.

Dong C, Davis RJ, Flavell, RA. 2002. MAP kinases in the immune response. Annu Rev Immunol 20:55–72.

Du G, Tu H, Li X, Pei A, Chen J, Miao Z, Li J, Wang C, Xie H, Xu X, Zhao H. 2014. Daphnetin, a natural coumarin derivative, provides the neuroprotection against glutamate-induced toxicity in HT22 cells and ischemic brain injury. Neurochem Res 39:269–275.

Figuera-Losada M, Rojas C, Slusher BS. 2014. Inhibition of microglia activation as a phenotypic assay in early drug discovery. J Biomol Screen 19:17–31.

Imani Fooladi AA, Mousavi SF, Seghatoleslami S, Yazdani S, Nourani MR. 2011. Toll-like receptors: Role of inflammation and commensal bacteria. Inflamm Allergy Drug Targets 10:198–207.

Jeong YH, Kim Y, Song H, Chung YS, Park SB, Kim HS. 2014. Anti-inflammatory effects of α-galactosylceramide analogs in activated microglia: Involvement of the p38 MAPK signaling pathway. PLoS ONE 9:e87030.

Kenny EF, O′Neill LA. 2008. Signalling adaptors used by Toll-like receptors: An update. Cytokine 43:342–349.

Kim SH, Smith CJ, Van Eldik LJ. 2004. Importance of MAPK pathways for microglial pro-inflammatory cytokine IL-1 beta production. Neurobiol Aging 25:431–439.

Kontogiorgis C, Detsi A, Hadjipavlou-Litina D. 2012. Coumarin-based drugs: A patent review (2008–present). Expert Opin Ther Pat 22:437–454.

Lee KM, Bang JH, Han JS, Kim BY, Lee IS, Kang HW, Jeon WK. 2013. Cardiotonic pill attenuates white matter and hippocampal damage via inhibiting microglial activation and downregulating ERK and p38 MAPK signaling in chronic cerebral hypoperfused rat. BMC Complement Altern Med 13:334.

Li Y, Gao C, Shi Y, Tang Y, Liu L, Xiong T, Du M, Xing M, Liu L, Yao P. 2013. Carbon monoxide alleviates ethanol-induced oxidative damage and inflammatory stress through activating p38 MAPK pathway. Toxicol Appl Pharmacol 273:53–58.

Lim GP, Chu T, Yang F, Beech W, Frautschy SA, Cole GM. 2001. The curry spice curcumin reduces oxidative damage and amyloid pathology in an Alzheimer transgenic mouse. J Neurosci 21:8370–8377.

Liu PW, Chen MF, Tsai AP, Lee TJ. 2012. STAT1 mediates oroxylin a inhibition of iNOS and pro-inflammatory cytokines expression in microglial BV-2 cells. PLoS ONE 7:e50363.

Lucas K, Maes M. 2013. Role of the Toll Like receptor (TLR) radical cycle in chronic inflammation: Possible treatments targeting the TLR4 pathway. Mol Neurobiol 48:190–204.

Mao X, Yin W, Liu M, Ye M, Liu P, Liu J, Lian Q, Xu S, Pi R. 2011. Osthole, a natural coumarin, improves neurobehavioral functions and reduces infarct volume and matrix metalloproteinase-9 activity after transient focal cerebral ischemia in rats. Brain Res 1385:275–280.

Marín-Teva JL, Cuadros MA, Martín-Oliva D, Navascués J. 2011. Microglia and neuronal cell death. Neuron Glia Biol 7:25–40.

Morales I, Guzmán-Martínez L, Cerda-Troncoso C, Farías GA, Maccioni RB. 2014. Neuroinflammation in the pathogenesis of Alzheimer′s disease. A rational framework for the search of novel therapeutic approaches. Front Cell Neurosci 8:112.

Park HY, Kim TH, Kim CG, Kim GY, Kim CM, Kim ND, Kim BW, Hwang HJ, Choi YH. 2013. Purpurogallin exerts anti-inflammatory effects in lipopolysaccharide-stimulated BV2 microglial cells through the inactivation of the NF-κB and MAPK signaling pathways. Int J Mol Med 32:1171–1178.

Perry VH, Holmes C. 2014. Microglial priming in neurodegenerative disease. Nat Rev Neurol 10:217–224.

Qi Z, Yin F, Lu L, Shen L, Qi S, Lan L, Luo L, Yin Z. 2013. Baicalein reduces lipopolysaccharide-induced inflammation via suppressing JAK/STATs activation and ROS production. Inflamm Res 62:845–855.

Qu WS, Tian DS, Guo ZB, Fang J, Zhang Q, Yu ZY, Xie MJ, Zhang HQ, Lü JG, Wang W. 2012. Inhibition of EGFR/MAPK signaling reduces microglial inflammatory response and the associated secondary damage in rats after spinal cord injury. J Neuroinflammation 9:178.

Raingeaud J, Gupta S, Rogers JS, Dickens M, Han J, Ulevitch RJ, Davis RJ. 1995. Pro-inflammatory cytokines and environmental stress cause p38 mitogen-activated protein kinase activation by dual phosphorylation on tyrosine and threonine. J Biol Chem 270:7420–7426.

Ren DY, Xu T, Li R, Huang C, Huang Y, Li RQ, Li HY, Li J. 2013. 5,7,3′-triacetyl hesperetin suppresses adjuvant-induced arthritis in rats through modulating JAK2/STAT3 pathway. Am J Chinese Med 41:601–614.

Ringman JM, Frautschy SA, Cole GM, Masterman DL, Cummings JL. 2005. A potential role of the curry spice curcumin in Alzheimer′s disease. Curr Alzheimer Res 2:131–136.

Riveiro ME, DeKimpe N, Moglioni A, Vázquez R, Monczor F, Shayo C, Davio C. 2010. Coumarins: Old compounds with novel promising therapeutic perspectives. Curr Med Chem 17:1325–1338.

Rock RB, Peterson PK. 2006. Microglia as a pharmacological target in infectious and inflammatory diseases of the brain. J Neuroimmune Pharmacol 1:117–126.

Rubio-Perez JM, Morillas-Ruiz JM. 2012. A review: Inflammatory process in Alzheimer′s disease, role of cytokines. Sci World J 2012:756357.

Saravanan S, Hairul I, Prakash VI, Babu N, Pandikumar P, Thirugnanasambantham K, Chellappandian M, Simon D, Raj C, Gabriel P, Ignacimuthu S. 2014. Swertiamarin attenuates inflammation mediators via modulating NF-kappaB/I kappaB and JAK2/STAT3 transcription factors in adjuvant induced arthritis. Eur J Pharm Sci 56:70–86.

Shu Z, Yang B, Zhao H, Xu B, Jiao W, Wang Q, Wang Z, Kuang H. 2014. Tangeretin exerts anti-neuroinflammatory effects via NF-κB modulation in lipopolysaccharide-stimulated microglial cells. Int Immunopharmacol 19:275–282.

Sun M, Hu J, Song X, Wu D, Kong L, Sun Y, Wang D, Wang Y, Chen N, Liu G. 2013. Coumarin derivatives protect against ischemic brain injury in rats. Eur J Med Chem 67:39–53.

Streit WJ, Xue QS. 2009. Life and death of microglia. J Neuroimmune Pharmacol 4:371–379.

Tanaka S, Ishii A, Ohtaki H, Shioda S, Yoshida T, Numazawa S. 2013. Activation of microglia induces symptoms of Parkinson′s disease in wild-type, but not in IL-1 knockout mice. J Neuroinflammation 10:143.

Tang CH, Yang RS, Chien MY, Chen CC, Fu WM. 2008. Enhancement of bone morphogenetic protein-2 expression and bone formation by coumarin derivatives via p38 and ERK-dependent pathway in osteoblasts. Eur J Pharmacol 579:40–49.

Wang S, Wang H, Jing H, Wang S, Kang L, Gao X, Hu L, Zheng X. 2012. Anti-inflammatory effects of isopropyl 3-(3, 4-dihydroxyphenyl)-2-hydroxypropanoate, a novel metabolite from danshen, on activated microglia. Chin J Physiol 55:428–434.

Yao L, Kan EM, Lu J, Hao A, Dheen ST, Kaur C, Ling EA. 2013. Toll-like receptor 4 mediates microglial activation and production of inflammatory mediators in neonatal rat brain following hypoxia: Role of TLR4 in hypoxic microglia. J Neuroinflammation 10:23.

Zeng KW, Wang S, Dong X, Jiang Y, Jin HW, Tu PF. 2014. Sesquiterpene dimmer (DSF-27) inhibits the release of neuroinflammatory mediators from microglia by targeting spleen tyrosine kinase (Syk) and Janus kinase 2 (Jak2): Two major non-receptor tyrosine signaling proteins involved in inflammatory events. Toxicol Appl Pharmacol 275:244–256.

Zhao H, Cheng L, Liu Y, Zhang W, Maharjan S, Cui Z, Wang X, Tang D, Nie L. 2014. Mechanisms of anti-inflammatory property of conserved dopamine neurotrophic factor: Inhibition of JNK signaling in lipopolysaccharide-induced microglia. J Mol Neurosci 52:186–192.

Zhi L, Ang AD, Zhang H, Moore PK, Bhatia M. 2007. Hydrogen sulfide induces the synthesis of proinflammatory cytokines in human monocyte cell line U937 via the ERK-NF-kappaB pathway. J Leukoc Biol 81:1322–1332.

SUPPORTING INFORMATION

Additional supporting information may be found in the online version of this article at the publisher's web-site.